Atmos. Chem. Phys. Discuss., https://doi.org/10.5194/acp-2017-1226
Manuscript under review for journal Atmos. Chem. Phys.
Discussion started: 16 January 2018

Atmospheric Chemistry and Physics Discussions

Foreign and domestic contributions to springtime ozone over China

Ruijing Ni[1], Jintai Lin[1], Yingying Yan[1], Weili Lin[2]

[1]Laboratory for Climate and Ocean-Atmosphere Studies, Department of Atmospheric and Oceanic Sciences, School of Physics, Peking University, Beijing 100871, China
[2]College of Life and Environmental Sciences, Minzu University of China, Beijing 100081, China

Correspondence to: J.-T. Lin (linjt@pku.edu.cn)

Abstract. China is facing a severe ozone problem, but the origin of its ozone remains unclear. Here we use a GEOS-Chem based global-regional two-way coupled model system to quantify the individual contributions of eight emission source regions worldwide to springtime ozone in 2008 over China. The model reproduces the observed ozone from 31 ground sites and various aircraft and ozonesonde measurements in China and nearby countries, with a mean bias at 10–15% both near the surface and in the troposphere. We then combine zero-out simulations, tagged ozone simulations, and a linear weighting approach to accounting for the effect of nonlinear chemistry on ozone source attribution. We find considerable contributions of total foreign anthropogenic emissions to surface ozone over China (2–11 ppb). For ozone averaged over China of anthropogenic origin, foreign regions together contribute 40–50% below the height of 2 km and 85% in the upper troposphere. For total foreign anthropogenic emissions contributed ozone over China at various heights, the portion of transboundary ozone produced within foreign emission source regions is less than 50%, with the rest produced by precursors transported out of those source regions. Japan and Korea contribute 0.6–2.1 ppb of surface ozone over the east coastal regions. South-East Asia contributes 1–5 ppb over much of southern China and South Asia contributes up to 5–10 ppb of surface ozone over border of southwestern China; and their contributions increase with height due to strong upwelling over the source regions. European contribution reaches 2.1–3.0 ppb for surface ozone over the northern border of China and 1.5 ppb in the lower troposphere averaged over China. North America contributes 0.9–2.7 ppb of surface ozone over most of China (1.5–2.1 ppb over the North China Plain), with a China average at 1.5–2.5 ppb at different heights below 8 km, due to its large anthropogenic emissions and the transport-favorable mid-latitude westerly. Global emission reduction is critical for China's ozone mitigation.

Atmos. Chem. Phys. Discuss., https://doi.org/10.5194/acp-2017-1226
Manuscript under review for journal Atmos. Chem. Phys.
Discussion started: 16 January 2018

1. Introduction

Ozone is an important atmospheric oxidant and the primary source of the hydroxyl radical (OH). At surface, ozone also damages human health and reduces crop yield. China is currently facing a severe ozone pollution problem, with measured maximum hourly ozone exceeding 200 ppb in many cities (Wang et al., 2006; Xue et al., 2014). Even in the remote areas of western China, measured daily mean concentrations of ozone exceed 50 ppb frequently (Xue et al., 2011; Lin et al., 2015). Xu et al. (2016) showed that daytime ozone at Waliguan, a global background station, grew significantly from 1994 to 2013 at a rate of 0.24 ± 0.16 ppb year^{-1}. The severe ozone problem is largely associated with growth in anthropogenic emissions of nitrogen oxides (NOx) and non-methane volatile organic compounds (NMVOC). Chinese anthropogenic NOx emissions increased at a rate of 7.9% year^{-1} from 2000 to 2010 (Zhao et al., 2013); and its anthropogenic NMVOC emissions increased from 22.45 Tg in 2008 to 29.85 Tg in 2012 (Wu et al., 2016).

Ozone has a lifetime of several days to weeks in the troposphere (Young et al., 2013; Yan et al., 2016), which makes its long-distance transport across regions and even continents possible. Many observational and modeling studies have showed substantial trans-Pacific and trans-Atlantic transport of ozone and precursors (Jacob et al., 1999; Derwent et al., 2004; Lin et al., 2008; Cooper et al., 2010; Verstraeten et al., 2016). The trans-Pacific transport of East Asian air pollutants enhances springtime surface ozone concentrations over the western United States by 1–5 ppb (Zhang et al., 2008; Brown-Steiner and Hess, 2011; Lin et al., 2012b; Lin et al., 2014). Auvray and Bey (2005) reported that North American and Asian ozone account for 10.9% and 7.7% of ozone over Europe, respectively. The Hemispheric Transport of Air Pollution (HTAP) project studied the trans-continental pollution, by model sensitivity simulations applying a 20% perturbation in anthropogenic emissions in four regions (North America, Europe, South Asia, and East Asia, each defined as a broad rectangle-shaped area) (HTAP, 2010). HTAP showed that the annual average impact of North American emissions on East Asian surface ozone is comparable to the impact of East Asian emissions on North America (0.22 ppb averaged over each rectangular region).

Several studies investigated the influence of transboundary transport on surface ozone over Chinese territory (Wang et al., 2011; Li et al., 2014; Li et al., 2016b; Zhu et al., 2016; Yin et al., 2017). Wang et al. (2011) used tagged ozone simulations with GEOS-Chem to study the global production of surface ozone over China for 2006. They showed that in spring 2006, tropospheric ozone produced over India contributed up to 6 ppb to surface ozone over western China; and that ozone produced over Europe and North America each contributed 2–5 ppb of ozone over northeastern China and North China. Using an emission zero-out method with MOZART simulations (i.e., without versus with emissions), Li et al. (2014) reported that modeled trans-Eurasian ozone

transport enhanced surface ozone over northwestern China by 2–6 ppb in spring 2000. Using tagged ozone simulations with MOZART, Zhu et al. (2016) revealed significant springtime ozone transport (~ 6 ppb) from Europe and Africa to Waliguan averaged from 1997 to 2007 and 3–5 ppb ozone from North and South America together. Using a tagged ozone method based on NAQPMS, Li et al. (2016) found 0.5–3.0 ppb of ozone over northeastern China produced over the Korean peninsula in 2010. Based on observational and back-trajectory analyses, Yin et al. (2016) found that ozone at the Nam Co site over Tibet in spring is greatly affected by anthropogenic contributions from South Asia.

Transboundary ozone due to precursor emissions of a source region can be produced both within and outside the source region. The two mechanisms contribute roughly equally for the case of trans-Pacific ozone from East Asia to the western United States (Zhang et al., 2008; Jiang et al., 2016). And the ozone production along the transport pathway is largely associated with thermal dissociation of peroxyacetyl nitrate (PAN) that has been formed in the boundary layer of the NOx emission source region. The transport of ozone precursors means that ozone produced within a region (from emitted and transported precursors worldwide) differs from ozone produced from that region's emissions. This difference affects how ozone over a receptor region is attributed to other regions (Wang et al., 2011; Li et al., 2014). It is thus important that the contribution of ozone produced at a "producing region" from emissions of a source region be quantified explicitly.

Here we simulate the contributions of anthropogenic emissions in individual regions across the globe to ozone at various heights over China. As typically assumed, anthropogenic contributions are associated with anthropogenic NOx, carbon monoxide (CO) and NMVOC emissions, excluding the effect of methane. We use a GEOS-Chem based two-way coupled modeling system (Yan et al., 2014; 2016) that integrates an Asian nested model and a global model in a sense of two-way exchange, which better simulates multi-scale interactions between the nested and global domains. Our study is focused on spring 2008, in which season a comprehensive set of ground, aircraft and ozonesonde measurements over China is available for model evaluation. Also, transboundary transport of ozone is most significant in spring due to active cyclonic activities and strong westerly winds (Liang et al., 2004; Wang et al., 2011; HTAP, 2010).

We explicitly identify ozone produced in 10 individual regions of the world from anthropogenic precursor emissions in each of eight source regions. For this purpose, we combine the emission zero-out method and the tagged ozone approach (Wang et al., 1998). The zero-out or similar emission perturbation methods are widely used to quantify the contribution of emissions in a source region to a receptor region as a combined result of the two production-transport mechanisms aforementioned (Lin et al., 2008; HTAP, 2010; Lin et al 2012a; Li et al., 2014). The tagged ozone approach quantifies the ozone produced in any designated region with no information about

whether the associated precursors are emitted in that region or are transported from somewhere else (Wang et al., 1998; Wang et al., 2011; Li et al., 2016b). To account for ozone production nonlinearity, we use a simple linear weighting method to adjusting simulation results, similar to Li et al. (2016a).

The rest of our paper is organized as follows. Section 2 presents model simulations, measurement data, and the ozone source attribution method. Section 3 evaluates the modeled ozone and CO using ground, aircraft and ozonesonde observations. Section 4 analyzes the modeled contributions to near-surface ozone over China by natural sources as well as anthropogenic emissions in individual regions. Section 5 shows the ozone source attribution at different heights of the troposphere. For each emission source region, it also separates the contribution of ozone produced within that source region from the contribution produced outside of that source region. Section 6 concludes the study.

2. Model simulations, measurements, and source attribution method

2.1 Two-way coupled GEOS-Chem modeling system

The two-way coupled system (Yan et al., 2014; Yan et al., 2016) is built upon version 9-02 of GEOS-Chem (http://wiki.seas.harvard.edu/geos-chem/index.php/Main_Page). Here we couple the global GEOS-Chem model (at 2.5° long. x 2° lat.) with its nested model covering Asia (70 °E–150 °E, 11 °S–55 °N, at 0.667° long. x 0.5° lat.). Through the PKUCPL two-way coupler, for every three hours the global model provides lateral boundary conditions for the nested model, while the nested model results replace the global model results within the nested domain (Yan et al., 2014; 2016). Both models are driven by the GEOS-5 assimilated meteorological fields at respective horizontal resolutions from National Aeronautics and Space Administration Global Modeling and Assimilation Office. There are 47 vertical layers for both models, and the lowest 10 layers are about 130 m thick each.

Both the global and nested GEOS-Chem models include the full gaseous HOx-Ox-NOx-CO-NMVOC chemistry (Mao et al., 2013) and online aerosol calculations, with further updates detailed in Lin et al. (2012) and Yan et al. (2016). As aromatics are not explicitly represented in the model, following Lin et al. (2012), we approximate the ozone production of aromatics by increasing anthropogenic emissions of propene by a factor of four, based on their reactivity differences, their similarity in emission spatial variability, and recently estimated emission amount of aromatics (Liu et al., 2010). We use the Linoz scheme for ozone production in the stratosphere (McLinden et al., 2000). We adjust the stratospheric production rate in the nested model to ensure that the stratosphere-troposphere exchange (STE) of ozone in the nested model matches the STE in the global model over the same nested domain (Yan et al., 2016). Vertical mixing in the planetary boundary layer (PBL) is parameterized by a non-local scheme

(Holtslag and Boville, 1993; Lin and McElroy, 2010), and convection in the model employs the relaxed Arakawa-Schubert scheme (Moorthi and Suarez, 1992).

Table 1 lists the emission inventories used here. Global anthropogenic emissions of NOx and CO in 2008 are from the Emission Database for Global Atmospheric Research (EDGAR v4.2). Anthropogenic NMVOC emissions are from the REanalysis of TROpospheric chemical composition (RETRO) inventory for 2000. Anthropogenic emissions over China, the rest of Asia, the United States, Canada, Mexico and Europe are replaced by regional inventories MEIC (for 2008), INTEX-B (for 2006), NEI2005 (for 2005), CAC (for 2008), BRAVO (for 1999) and EMEP (for 2007), respectively. Emissions of CO and NOx are scaled to 2008 in the United States and to 2006 in Mexico. (http://wiki.seas.harvard.edu/geos-chem/index.php/Scale_factors_for_anthropogenic_emissions). We use daily biomass burning emissions from Global Fire Emission Database version 3 (GFED3) (van der Werf et al., 2010). Biogenic emissions of NMVOC are calculated online based on the MEGAN v2.1 scheme (Guenther et al., 2012). For lightning NOx emissions, flash rates are calculated based on the cloud top height and constrained by climatological satellite observations (Murray et al., 2012), and the vertical profile of emitted NOx follows Otto et al. (2010). Online calculation of soil NOx emissions follows Hudman et al. (2012).

2.2 Zero-out simulations, tagged ozone simulations, and weighted adjustment

Table 2 presents 10 full-chemistry simulations to quantify Chinese and foreign anthropogenic contributions to springtime ozone over China in 2008. A base simulation (CTL) includes all emissions. The second simulation excludes anthropogenic NOx, CO and NMVOC emissions worldwide to determine the natural ozone (xANTH). Eight additional simulations exclude anthropogenic emissions over China (xCH), Japan and Korea (xJAKO), South-East Asia (xSEA), South Asia (xSA), Rest of Asia (xROA), Europe (xEU), North America (xNA) and Rest of World (xROW), respectively (see regional definitions in Fig. 1). All simulations cover November 2007 through May 2008, with the first four months used for spin-up, except for additional CTL simulations in other years for model evaluation purposes.

Table 2 also shows 10 tagged simulations (denoted as T_CTL, T_xANTH, etc.) with respect to CTL and other eight zero-out sensitivity simulations. Each tagged simulation includes 10 tracers to track ozone produced within the eight source regions, produced within the oceanic region, or transported from the stratosphere. Considering the time for STE of air, all tagged ozone simulations are spun up for 10 years.

Ozone production is nonlinearly dependent on its precursors, adding uncertainties to the source attribution calculated by emission perturbation methods (Wu et al., 2009). To account for this issue, we use a linear weighting method to adjust all ozone attribution results (Li et al., 2016a), unless stated otherwise. Equation 1 is an example to determine the contribution from Chinese anthropogenic emissions (here Ci represents the sensitivity simulation for one of the eight emission source regions). The

adjustment is done for each grid cell over China.

$$C_{CH} = \frac{Con(CTL)}{\sum_{i=1}^{8}[Con(CTL)-Con(Ci)]+Con(xANTH)} \times [Con(CTL) - Con(xCH)] \quad (1)$$

2.3 Measurements

This study presents model evaluation over China and its neighboring countries in spring. We also evaluate the simulation of CO, a relatively long-lived transport tracer. Figure 3 shows the suite of ground, aircraft and ozonesonde measurements.

2.3.1 Surface measurements

Measurements from a total of 32 ground sites are used here; see Tables 3 and 4 for geographical information. Routine observations of ozone and CO in China were scarcely available before 2013. Hourly data are available for this study from five rural/background sites across China maintained by the Chinese Meteorological Administration (Xu et al., 2008; Lin et al., 2009; Fang et al., 2014; Ma et al., 2014). These sites include a rural site (Gucheng over North China Plain), three regional background sites (Longfengshan over the northeast, Lin'an over the east, and Shangri-La over the southwest), and a Global Atmosphere Watch (GAW) background site (Waliguan over the west). Data are available for 2007 at Gucheng and Longfengshan and for 2008 at other three sites.

We also use hourly ozone and CO measurements in spring 2008 from six GAW background sites in the vicinity of China from the World Date Center for Greenhouse Gases (WDCGG, http://ds.data.jma.go.jp/gmd/wdcgg/cgi-bin/wdcgg/catalogue.cgi). These sites include Issyk-Kul in Kyrgyzstan, Everest-Pyramid in Nepal, Bukit Koto Tabang in Indonesia, and Yonagunijima, Tsukuba and Ryori in Japan.

To obtain a more comprehensive observation dataset for model evaluation, we further use monthly mean ozone data in spring 2008 from 15 remote/rural sites from the Acid Deposition Monitoring Network in East Asia (EANET, http://www.eanet.asia/product/index.html). We also collect monthly ozone observation data at six sites over China from the literature, including data at three mountain sites (Mts. Tai, Hua, and Huang).

2.3.2 Measurements of vertical profiles

To evaluate vertical distribution of ozone and CO over China, we use observations from the Measurements of Ozone and Water Vapor by Airbus In-Service Aircraft (MOZAIC) program (Marenco et al., 1998). Data during both ascending and descending processes of the aircrafts are available during spring 2000–2005 at three airports (Beijing, Shanghai, and Hong Kong). The vertical resolution is 150 m.

We further use the ozonesonde data at six sites in spring 2008 from the World Ozone

and Ultraviolet Date Center (WOUDC, http://www.woudc.org/data/explore.php?lang=en) operated by the Meteorological Service of Canada. The six sites include Hanoi in Vietnam, Hong Kong in China, Sepang Airport in Malaysia, and Sapporo, NAHA and Tateno in Japan. Ozonesondes are launched every few days, thus the data are relatively scarce. We also use the GPSO3 ozonesonde data in spring 2008 over Beijing measured by the Institute of Atmospheric Physics (IAP) of the Chinese Academy of Sciences (Wang et al., 2012). All ozonesonde measurements were launched at around 14:00 local time.

3. Model evaluation

Here we focus on model evaluation over China and its neighboring area in spring. Global ozone evaluation of the two-way coupled model system is detailed in Yan et al. (2016) using 1420 ground sites, various aircraft observations and satellite measurements, although the observations over China are sparse.

3.1 Surface ozone and CO over China and nearby countries

Figure 3 compares the springtime time series of modeled (solid red line) and observed (solid black line) maximum daily average 8-hour (MDA8) ozone concentrations at 10 sites with daily measurements. Model data are sampled at times and locations coincident with valid observations.

Figure 3a–b evaluates the model results at Gucheng and Longfengshan. To compare to observations in spring 2007 at these two sites, we conduct an additional full chemistry simulation for 2007. At these sites, the model captures the observed MDA8 ozone, with a normalized mean bias (NMB) of 2% at Gucheng and 4% at Longfengshan. The respective correlation coefficients (R) for day-to-day variability are 0.51 and 0.59; the modest correlation is primarily because the model does not capture a few short-term spikes.

At Lin'an (Fig. 3c), the modeled spring average MDA8 ozone matches the observed value (68.9 ppb versus 65.1 ppb, R = 0.64). The model cannot reproduce the observed extreme low values on several days. This deficiency is likely due to representative errors of model meteorology. Located in a hilly area, this site often receives rains and fogs in spring, which is not captured by the model meteorology at a resolution of 0.667° long. x 0.5° lat. We find that the extremely low observed ozone values normally occur on days with high relative humidity (black dashed line, reflecting rainy or foggy days), when the model underestimates RH (red dashed line) and overestimates ozone.

At Shangri-La, Waliguan and Issyk-Kul (Fig. 3d–f), with high latitudes and little local anthropogenic sources, the model overestimates the MDA8 ozone by 7–8 ppb (11–14%). At Everest-Pyramid in Nepal (Fig. 3g), the overestimate reaches 13 ppb (19%). These positive biases are due to overestimated transport from the free troposphere and stratosphere. The model captures the temporal variability of MDA8 ozone quite well

(R = 0.72–0.78) at the three Japanese sites (Yonagunijima, Tsukuba and Ryori, Fig. 3h–j). Its NMB is within 2% at Yonagunijima and Ryori. There is an overestimate at Tsukuba (NMB = 18%), mostly reflecting the large positive biases on a few days.

Table 4 shows model comparisons with monthly mean EANET ozone data. These data represent daily mean rather than MDA8 values, based on the availability of observations. At seven sites, the model results exceed the observations with a mean difference by 7 ppb (16%). At the other eight sites, the model results are smaller than the observations with a mean difference by 7 ppb (11%). These differences reflect model biases as well as a sampling bias due to lack of knowledge on which days contain valid observations.

Table 4 further compares the modeled monthly mean daily mean ozone in spring 2008 to the observations in various years collected from the literature. Again, the comparison is affected by a sampling bias. The model reproduces the average magnitude of ozone at the three mountainous sites (Mts. Tai, Hua and Huang) with a mean bias below 5 ppb (9%). The model has a large overestimate by 48% at the rural site in Hong Kong, although times are different (2008 versus 1994–2007). The model overestimates ozone at an urban site in Nanjing by 16%, although the observations were made in 2000–2002 when Chinese anthropogenic emissions of NOx were only about half of those in 2008 (Xia et al., 2016).

We also evaluate the modeled daily average CO at six sites within and outside China with available hourly observations (Fig. 4). Overall, the model captures the day-to-day variability of daily mean CO fairly well (R = 0.40 at Lin'an, 0.60 at Shangri-La, 0.56 at Ryori, and 0.73–0.82 at other three sites). It has a small mean bias (within 3%) at Bukit Koto Tabang and Ryori, although with negative biases (by 13–33%) at other four sites. Such an underestimate is typical in global simulations (Young et al., 2013), and it may be related to excessive OH (Young et al., 2013; Yan et al., 2014; 2016) and/or underestimated emissions (Kopacz et al., 2010; Wang et al., 2011). As compared to the coarse-resolution global model alone, our two-way coupling results in less CO underestimate (Yan et al., 2014), although it does not eliminate the bias.

3.2 Vertical profiles of ozone and CO

Figure 5a–c compares modeled ozone in 2008 to MOZAIC data over 2000–2005 at the airports of Beijing, Shanghai and Hong Kong. Although model and MOZAIC data are in different years, to achieve best sampling consistency, we sample the model results at times of day when the commercial aircrafts take off or land in with available MOZAIC data. The timing information is shown in Fig. 5. GEOS-Chem reproduces the vertical gradient of MOZIAC ozone in general. The model underestimates MOZIAC ozone in the PBL over Beijing Airport mainly due to inconsistent temporal sampling, as further comparison with GPSO3 ozonesonde data (Bian et al., 2007; Wang et al., 2012), where model results are sampled at times coincident with the observations, shows little model bias (within 4%, Fig. 5g). Over Hong Kong, the model captures the weak vertical

gradient between 2 km and 11 km, although it has a positive bias below 2 km due to its inability to capture the complex terrains and local pollution source characteristics around the airport. The model overestimates ozone in the middle and upper troposphere over Shanghai, with larger biases at higher altitudes, likely indicating too strong STE. Other causes may include differences in meteorology and emissions between 2000–2005 and 2008.

Figure 6 compares the modeled ozone profiles to WOUDC data at six sites. Here model results are sampled at ozonesonde launch times, and ozonesonde data are regridded to match the model vertical resolution. Overall, GEOS-Chem captures the vertical gradient of ozone fairly well. The model reproduces the overall weak vertical gradients at Hanoi, Hong Kong, Sepang and NAHA. It also reproduces the rapid increases above 8 km at Sapporo and Tateno, although it has positive biases at 10–20 ppb. GEOS-Chem reproduces the observed middle and upper tropospheric ozone at Hong Kong and Sepang, although it has an overestimate in the lower troposphere, consistent with the bias shown in Fig. 5c.

Figure 5d–f also compares the modeled CO with the MOZAIC data. Similar to the evaluation results for surface CO, GEOS-Chem generally underestimates the MOZAIC CO at most heights above the three airports, although it captures the vertical shape fairly well.

3.3 Summarizing remark on model evaluation

Our simulation has a small NMB for surface ozone, at about 10% averaged over 10 sites with hourly data (Fig. 3 and Table 3) and about 15% averaged over 21 sites with monthly data from EANET and the literature (Table 4). The model also captures the general vertical distribution of ozone at ten places over China and nearby regions, with a tropospheric mean bias at 12%. These agreements allow using the model for source attribution studies in the next sections. On the other hand, with a horizontal resolution of about 50 km over Asia, the model often fails to simulate the complex terrains, local meteorological conditions, and/or local emission characteristics at several hilly or airport sites. The model also tends to overestimate the STE influences over Asia. Addressing these issues warrant future research with improved model resolutions and STE representation.

GEOS-Chem tends to underestimate CO over Asia (by 20% on average), similar to many other models (Kopacz et al., 2010; Young et al., 2013). We conduct a sensitivity simulation by doubling Chinese anthropogenic CO emissions, which result in a slight increase in surface ozone by 0.1–0.4 ppb and 2–3 ppb over clean and polluted areas of China, respectively. The low sensitivity of ozone to CO emissions were also found by Jiang et al. (2015). We thus conclude that our ozone simulations over China are influenced insignificantly by the underestimate in CO.

Atmos. Chem. Phys. Discuss., https://doi.org/10.5194/acp-2017-1226
Manuscript under review for journal Atmos. Chem. Phys.
Discussion started: 16 January 2018

4. Source attribution modeling for surface ozone over China

4.1 Total, background and natural ozone

Figure 7a shows the modeled spatial distribution of near-surface daily mean ozone in spring 2008 over China from all natural and anthropogenic sources, i.e., the CTL case. Ozone concentrations reach 75–80 ppb over the southern Tibetan Plateau, and they are minimum (25–40 ppb) over the North China Plain and many populous cities across eastern China. Ozone are about 45–60 ppb over the vast southeast, northwest and northeast.

The simulated natural ozone (i.e., without anthropogenic emissions worldwide, the xANTH case) shows a strong gradient from the southern Tibetan Plateau (65–75 ppb) to the northwest (35–40 ppb) and the east (20–35 ppb) (Fig. 7c). Wang et al. (2011) shows similar gradients of nature ozone in 2006. Natural ozone contribute 80–90% of total surface ozone over Tibet and the northwest with low local anthropogenic emissions. The large natural ozone concentrations over Tibet are a result of vertical transport from the free troposphere and stratosphere due to its high altitudes and hilly terrains (that are conducive to vertical exchange) (Ding and Wang, 2006;Lin et al., 2015;Xu et al., 2017). They pose potential threats for public health and ecosystems there.

The simulated background ozone (i.e., without Chinese anthropogenic emissions, the xCH case) is shown in Fig. 7b. The background ozone are higher than the natural ozone by 2–11 ppb over most Chinese regions (Fig. 8b). This indicates large influences of foreign anthropogenic emissions through atmospheric transport of ozone and its precursors, as discussed in detail below.

4.2 Domestic versus foreign anthropogenic contributions to ozone

Figure 8a shows the spatial distribution of domestic anthropogenic contributions to daily mean surface ozone over China (CTL − xCH, as adjusted with Eq. 1). Over most of the west and northeast, Chinese anthropogenic emissions are relatively low, and they result in ozone concentrations by 0–4 ppb. In contrast, domestic contributions reach 16–25 ppb over the south due to more emissions and favorable conditions for photochemistry. Over the North China Plain and many populous cities, Chinese anthropogenic emissions lead to reductions (instead of enhancements) of surface ozone. This is because of a weak ozone production efficiency and a strong titration effect by excessive domestic NOx emissions. Figure 8d-f shows that when Ox (= O_3 + NO_2) is considered, Chinese anthropogenic contributions vary from 2–4 ppb over the west to 6–12 ppb over the North China Plain and to 20–35 ppb over the southeast (Fig. 8d).

Figure 8b shows the simulated contributions to Chinese surface ozone by all foreign anthropogenic emissions. Foreign contributions reach 7–11 ppb along much of Chinese

borders, and they exceed 6 ppb over the vast northern regions. The foreign contribution reduces from the border to the inner areas, with a minimum (2–3 ppb) over the Sichuan Basin where the air is more isolated. In terms of anthropogenic ozone, foreign contributions account for up to 90% over most of western and northeastern China (Fig. 8c), consistent with the findings by Li et al. (2015) for western China in 2000. Foreign anthropogenic contributions to Ox over China are similar to their contributions to ozone (Fig. 8e), except at places with strong Chinese NOx emissions that lead to titration of ozone.

Figure 9 further shows the contributions to Chinese surface ozone by anthropogenic emissions in seven individual foreign regions. The pattern of influence differs among these source regions due to differences in the location of source region, emission magnitude, pollutant lifetimes and transport pathways. Anthropogenic emissions in Japan and Korea result in 0.6–2.1 ppb of ozone enhancement along the Chinese coast. The tagged ozone simulation with NAQPMS by Li et al. (2016) also showed that about 0.5–3.0 ppb of ozone over northeastern China in spring 2010 were produced over Korea peninsula, although there is a difference between ozone produced over a region and ozone produced from that region's emissions. Emissions from South-East Asia contribute 1–5 ppb over much of the southern provinces. Emissions from South Asia mostly affect southwestern China and Tibet (by up to 5-10 ppb over the border), due to effective transport by strong southwesterly associated with the Indian Monsoon. The "Rest of Asia" consists of many countries to the west of China, whose total contributions are about 2–5 ppb over much of northwestern China.

European anthropogenic emissions contribute 2.1–3.0 ppb of ozone along the northern border of China. The contributions decrease southwards, and are above 1 ppb over half of Chinese land areas. The MOZART simulation by Li et al. (2015) also showed a European contribution by 2 ppb to surface ozone over North China in 2000. North American anthropogenic emissions increase ozone by 1.8–2.7 ppb over much of western China, by 1.5–2.1 ppb over the populous North China Plain, and by less than 0.9 ppb over the south. The contributions are smaller than springtime Asian anthropogenic influences on western North America (e.g., 1–5 ppb averaged over 2001–2005 (Brown-Steiner and Hess, 2011b)), although the affected population is larger by roughly an order of magnitude.

Influences from "Rest of World" are about 0.6–1.2 ppb over Tibet and smaller over other Chinese land territory. The larger values over Tibet reflect its higher altitude and greater sensitivity to long-range transport via the free troposphere.

Figure 10a further highlights the largest foreign contributor to surface anthropogenic ozone at each location of China. North America is the largest foreign contributor over about half of Chinese land territory, including the populated North China Plain. Europe is the largest foreign contributor for the vast northeastern region, Rest of Asia for the western border region, South Asia for southwestern China, South-East Asia for southern China, and Japan and Korea for the eastern coast of China.

Atmos. Chem. Phys. Discuss., https://doi.org/10.5194/acp-2017-1226
Manuscript under review for journal Atmos. Chem. Phys.
Discussion started: 16 January 2018

5. Vertical distributions of domestic and foreign anthropogenic contributions

Figure 11a shows the domestic and foreign anthropogenic contributions to daily mean ozone at different heights above the ground averaged over China. The black line shows that Chinese emissions contribute 6.0–10.5 ppb of ozone below 2 km over China, with a maximum value at 0.7 km. This average amount of contribution reflects compensation between positive values over most regions and negative values over the North China Plain and many populous cities (see Sect. 4.2). Above 0.7 km, Chinese contribution decreases rapidly until 3 ppb at 5 km, above which height the contribution declines slowly until a value at 1 ppb at 12 km. By comparison, Chinese contribution to Ox is about 7–11 ppb below 2 km, and at higher altitudes the contribution is almost identical to that for ozone (not shown). The small contributions above 2 km for both ozone and Ox are because as ozone and precursors associated with Chinese emissions are lifted to higher altitudes, they are transported out of Chinese territory and destroyed gradually.

The grey line in Fig. 11a shows that the total foreign contribution is about 5.2–7.8 ppb at different heights with a reverse "C" shape, i.e., higher values at 3–9 km and lower values above or below that layer. The foreign contribution exceeds Chinese contribution at all heights above 2 km. Nonetheless, the total (Chinese + foreign) anthropogenic ozone is less than one third of natural ozone throughout the troposphere. Figure 10b shows that of ozone over China produced from all anthropogenic emissions, foreign emissions together contribute 50% at the surface, 40% at 0.7 km as a minimum, and 85% in the upper troposphere.

Figure 11b specifies the contribution of each foreign emission source region. Figure 11c further separates the portion of ozone produced within each source region's territory from the portion produced outside of that source region. South-East Asian contribution is about 0.5–2.5 ppb averaged over China, and it increases with height due to strong upwelling that lifts pollutants to the middle and upper troposphere. The contribution from Japan and Korea is below 0.5 ppb throughout the troposphere averaged over China (Fig. 11b). The share of transboundary ozone produced within South-East Asian territory and transported to China is about 10–45% (mostly below 30%), and the share for ozone produced within Japan and Korea is even smaller (5–25%) (Fig. 11c), highlighting the importance of ozone produced by precursors transported out of these two emission source regions.

South Asian contribution is only about 0.5–1.2 ppb throughout the troposphere (Fig. 11b). Although South Asia has more anthropogenic emissions than South-East Asia (Table 2), its contribution to ozone over China is smaller due to blocking of transport by the Himalayas with high elevation (Fig. 2). In addition, the share of transboundary ozone produced within South Asian territory reaches 70–90% below 6 km but declines rapidly to 28% at 12 km (Fig. 11c), a characteristic drastically different from the share for South-East Asia.

462 The contribution from Rest of Asia is below 1.8 ppb at all heights with a negative
463 vertical gradient (Fig. 11b). Above 3 km, the portion of transboundary ozone produced
464 within the territory of Rest of Asia is similar to that for South Asia (Fig. 11c). However,
465 the portion exhibits a strong vertical gradient below 3 km, with a minimum value at 45%
466 near the ground.

467 European contribution declines from 1.5 ppb in the lower troposphere to 0.2 ppb at 12
468 km, similar to that for Rest of Asia (Fig. 11b). In spring, Eurasian frontal activities
469 transport and gradually lift European pollutants to downwind areas. The portion of
470 transboundary ozone produced within European territory is about 55–65% at 3–10 km
471 but is as low as 20% below 1 km (Fig. 11c), suggesting that most Europe-contributed
472 near-surface ozone over China are produced from precursors transported out of Europe.

473 Figure 11b shows that North American anthropogenic emissions contribute about 1.5–
474 2.5 ppb of ozone below 8 km, although the contribution declines rapidly to 0.2 ppb at
475 12 km. Compared to Europe, North America is further away from China, but its
476 pollutants can be transported via the strong mid-latitude westerly. Averaged over China,
477 North American contribution is larger than European contribution at all heights, e.g.,
478 by a factor of two in the middle and upper troposphere. The higher contribution is due
479 to much more anthropogenic emissions in North America than in Europe. Table 3 shows
480 that North America emits NMVOC nearly twice as much as Europe does; and Wu et al.
481 (2009) showed that the amount of transboundary ozone is nearly proportional to
482 NMVOC emissions of the source region. In addition, Fig. 11c shows that the portion of
483 transboundary ozone produced within North American territory is only about 5–20%
484 below 8 km, reflecting the dominant contribution by ozone produced from transported
485 precursors. The low share of ozone produced within North America is primarily
486 because most of such ozone is destroyed during the transport from North America to
487 China (for about two weeks), given the tropospheric lifetime of ozone at about three
488 weeks (Yan et al., 2016).

489 The grey line in Fig. 11c shows the average portion of transboundary ozone from all
490 foreign source regions that is produced within the territories of respective foreign
491 regions. The average portion is less than 50% throughout the troposphere, is about 40%
492 at 2 km, and is as low as 25% near the surface. This again highlights the dominant
493 importance of ozone production along with the transport of precursors.

494 **6. Conclusions**

495 This study uses a GEOS-Chem based two-way coupled modeling system to simulate
496 Chinese and foreign anthropogenic contributions to springtime ozone at different
497 heights over China. Anthropogenic contributions are associated with anthropogenic
498 NOx, CO and NMVOC emissions, excluding the effect of methane. We combine the
499 zero-out simulations and tagged ozone simulations to separate the transboundary ozone
500 produced within the territory of each emission source region from the ozone produced
501 by anthropogenic precursors transported out of that source region. We use a weighting

approach to accounting for the effect of nonlinear ozone chemistry on source attribution estimates. Model evaluation using a suite of ground, aircraft and ozonesonde measurements show an overall small bias for ozone near the surface and in the troposphere (10% at 10 surface sites with hourly measurements, 15% at 21 surface sites with monthly observations, and 12% for vertical profiles). The model underestimates CO by 20% on average over China and nearby areas, which however does not affect the simulated ozone significantly.

Model simulations reveal that both total and natural ozone near the surface over China show a decreasing gradient from the southern Tibetan Plateau to the northwest and the east. Natural ozone contribute 80–90% of total surface ozone over Tibet and the northwest with low local anthropogenic emissions. Chinese anthropogenic emissions enhance surface ozone concentrations by 0–4 ppb over most of the west and northeast due to low emissions and by 16–25 ppb over the south due to more emissions and chemically conducive conditions. Chinese anthropogenic emissions result in reduced ozone, albeit with enhanced Ox, over the North China Plain and many populous cities, as a result of weak ozone production efficiency and strong titration by excessive Chinese NOx emissions.

Near the surface, foreign anthropogenic emissions contribute 2–11 ppb of Chinese ozone, with peak contributions at 7–11 ppb over the border and coastal regions of China. Over western and northeastern China, foreign emissions account for up to 90% of ozone of anthropogenic origin. Anthropogenic emissions in Japan and Korea result in 0.6–2.1 ppb of ozone along the Chinese coast. Emissions in South-East Asia contribute 1–5 ppb over much of southeastern China. South Asian emissions mostly affect southwestern China and Tibet (by up to 5 ppb), due to effective transport by strong southwesterly associated with the Indian Monsoon. European anthropogenic emissions contribute 2.1–3 ppb along the northern border of China and the contribution decreases southwards. North American anthropogenic emissions increase ozone by 1.8–2.7 ppb over much of the west, by 1.5–2.1 ppb over the populous North China Plain, and by less than 0.9 ppb over the south.

Vertically, for ozone of anthropogenic origin averaged over China, Chinese emissions contribute ~ 6 ppb (50%) of ozone at the surface, 6.0–10.5 ppb below 2 km, decreasing to 3 ppb at 5 km and 1 ppb at 12 km. The total foreign contribution increases from 40–50% below 2 km to 50–85% above that height. The contribution from Japan and Korea is below 0.5 ppb throughout the troposphere averaged over China. Despite its large emissions, South Asia contributes only about 0.5–1.2 ppb throughout the troposphere due to blocking of transport by the Himalayas. South-East Asian contribution increases with height due to strong upwelling that lifts pollutants to the upper troposphere. On the contrary, European contributions decreases from 1.5 ppb in the lower troposphere to 0.2 ppb at 12 km. Despite the long transport distance, North American contribution reaches as much as 1.5–2.5 ppb below 8 km due to its large anthropogenic emissions and the strong mid-latitude westerly favorable for transboundary transport.

For ozone of foreign anthropogenic origin averaged over China, the portion of transboundary ozone produced within foreign source regions is less than 50% throughout the troposphere, albeit with a strong vertical variability, indicating the importance of ozone produced by precursors transported out of those source regions. The portion also differs among each foreign source region of South-East Asia (10–45%) and Japan and Korea (5–25%), South Asia (from 70–90% below 6 km to 28% at 12 km), Europe (from 20% below 1 km to 55–65% at 3–10 km), and North America (5–20% below 8 km). Thus tracing ozone produced within the territory of a particular region is drastically different from tracing ozone associated with emissions in that region.

In summary, although China is a major pollutant emitter, the ozone above its territory consists primarily of natural sources, especially over western China with low local anthropogenic emissions. Moreover, for ozone of anthropogenic origin, a large portion results from foreign emissions, as analyzed here for spring 2008. In more recent years, Chinese anthropogenic NOx emissions have undergone a rapid decline as a result of domestic emission control (Xia et al., 2016), along with continuous reductions in North America and Western Europe (Yan et al., 2017a; 2017b) and changes in other regions. Future research is needed to quantify the resulting changes in ozone and its geographical origin. In addition, this study does not account for that a substantial portion of anthropogenic emissions in any region are associated with economic production for foreign consumption (Lin et al., 2014; Jiang et al., 2015a), which would affect how pollution is attributed to individual producing or consuming regions (Guan et al., 2014; Lin et al., 2016; Zhang et al., 2017). Nevertheless, our study suggests the great importance of global collaboration on emission reduction to mitigate ozone pollution in addition to domestic emission control efforts.

Acknowledgments

This research is supported by the National Natural Science Foundation of China (41775115) and the 973 program (2014CB441303). We acknowledge Dr. Chen Hongbin's team at IAP LAGEO for providing the GPSO3 ozonesonde data. We acknowledge the free use of ozone data from WDCGG (http://ds.data.jma.go.jp/gmd/wdcgg/), EANET (http://www.eanet.asia/product/index.html), WOUDC (http://www.woudc.org/data/explore.php?lang=en), and MOZAIC-IAGOS (http://www.iagos.fr/web/). We thank the European Commission for the support to the MOZAIC project (1994–2003) and the preparatory phase of IAGOS (2005–2012) partner institutions of the IAGOS Research Infrastructure (FZJ, DLR, MPI, KIT in Germany, CNRS, CNES, Météo-France in France and University of Manchester in United Kingdom), ETHER (CNES-CNRS/INSU) for hosting the database, the participating airlines (Lufthansa, Air France, Austrian, China Airlines, Iberia, Cathay Pacific) for the transport free of charge of the instrumentation.

583 **References**

584 Auvray, M., and Bey, I.: Long-range transport to Europe: Seasonal variations and
585 implications for the European ozone budget, J. Geophys. Res.-Atmos., 110,
586 10.1029/2004jd005503, 2005.
587 Bian, J. C., Gettelman, A., Chen, H. B., and Pan, L. L.: Validation of satellite ozone
588 profile retrievals using Beijing ozonesonde data, J. Geophys. Res.-Atmos., 112,
589 11, 10.1029/2006jd007502, 2007.
590 Bond, T. C., Bhardwaj, E., Dong, R., Jogani, R., Jung, S., Roden, C., Streets, D. G.,
591 and Trautmann, N. M.: Historical emissions of black and organic carbon aerosol
592 from energy-related combustion, 1850–2000, Global Biogeochem. Cy., 21,
593 GB2018, doi:10.1029/2006GB002840, 2007.
594 Brown-Steiner, B., and Hess, P.: Asian influence on surface ozone in the United States:
595 A comparison of chemistry, seasonality, and transport mechanisms, J. Geophys.
596 Res.-Atmos., 116, 13, 10.1029/2011jd015846, 2011.
597 Cooper, O. R., Parrish, D. D., Stohl, A., Trainer, M., Nedelec, P., Thouret, V., Cammas,
598 J. P., Oltmans, S. J., Johnson, B. J., Tarasick, D., Leblanc, T., McDermid, I. S.,
599 Jaffe, D., Gao, R., Stith, J., Ryerson, T., Aikin, K., Campos, T., Weinheimer, A.,
600 and Avery, M. A.: Increasing springtime ozone mixing ratios in the free
601 troposphere over western North America, Nature, 463, 344-348,
602 10.1038/nature08708, 2010.
603 Derwent, R. G., Stevenson, D. S., Collins, W. J., and Johnson, C. E.: Intercontinental
604 transport and the origins of the ozone observed at surface sites in Europe,
605 Atmospheric Environment, 38, 1891-1901, 10.1016/j.atmosenv.2004.01.008,
606 2004.
607 Ding, A. J., and Wang, T.: Influence of stratosphere-to-troposphere exchange on the
608 seasonal cycle of surface ozone at Mount Waliguan in western China, Geophysical
609 Research Letters, 33, 4, 10.1029/2005gl024760, 2006.
610 Fang, S. X., Zhou, L. X., Tans, P. P., Ciais, P., Steinbacher, M., Xu, L., and Luan, T.:
611 In situ measurement of atmospheric CO2 at the four WMO/GAW stations in China,
612 Atmospheric Chemistry and Physics, 14, 2541-2554, 10.5194/acp-14-2541-2014,
613 2014.
614 Guan, D., Su, X., Zhang, Q., Peters, G. P., Liu, Z., Lei, Y., and He, K.: The
615 socioeconomic drivers of China's primary PM2. 5 emissions, Environmental
616 Research Letters, 9, 024010, 2014.
617 Geng, G. N., Zhang, Q., Martin, R. V., Lin, J. T., Huo, H., Zheng, B., Wang, S. W., and
618 He, K. B.: Impact of spatial proxies on the representation of bottom-up emission
619 inventories: A satellite-based analysis, Atmospheric Chemistry and Physics, 17,
620 4131-4145, 10.5194/acp-17-4131-2017, 2017.
621 Guenther, A. B., Jiang, X., Heald, C. L., Sakulyanontvittaya, T., Duhl, T., Emmons, L.
622 K., and Wang, X.: The Model of Emissions of Gases and Aerosols from Nature
623 version 2.1 (MEGAN2.1): an extended and updated framework for modeling
624 biogenic emissions, Geoscientific Model Development, 5, 1471-1492,
625 10.5194/gmd-5-1471-2012, 2012.

626 Holtslag, A. A. M., and Boville, B. A.: LOCAL VERSUS NONLOCAL BOUNDARY-
627 LAYER DIFFUSION IN A GLOBAL CLIMATE MODEL, Journal of Climate,
628 6, 1825-1842, 10.1175/1520-0442(1993)006<1825:lvnbld>2.0.co;2, 1993.
629 HTAP: Hemispheric Transport of Air Pollution 2010 Executive Summary
630 ECE/EB.AIR/2010/10 Corrected, United Nations, available at:
631 http://www.htap.org/publications/2010_report/2010_Final_Report/EBMeeting20
632 10.pdf (last access: 1 February 2015), 2010.
633 Hudman, R. C., Moore, N. E., Mebust, A. K., Martin, R. V., Russell, A. R., Valin, L.
634 C., and Cohen, R. C.: Steps towards a mechanistic model of global soil nitric oxide
635 emissions: implementation and space based-constraints, Atmospheric Chemistry
636 and Physics, 12, 7779-7795, 10.5194/acp-12-7779-2012, 2012.
637 Jacob, D. J., Logan, J. A., and Murti, P. P.: Effect of rising Asian emissions on surface
638 ozone in the United States, Geophysical Research Letters, 26, 2175-2178,
639 10.1029/1999gl900450, 1999.
640 Jiang, X., Zhang, Q., Zhao, H., Geng, G., Peng, L., Guan, D., Kan, H., Huo, H., Lin, J.-
641 T., Brauer, M., Martin, R. V., and He, K.: Revealing the hidden health costs
642 embodied in Chinese exports, Environmental Science & Technology,
643 10.1021/es506121s, 2015a.
644 Jiang, Z., Worden, J. R., Jones, D. B. A., Lin, J. T., Verstraeten, W. W., and Henze, D.
645 K.: Constraints on Asian ozone using Aura TES, OMI and Terra MOPITT,
646 Atmospheric Chemistry and Physics, 15, 99-112, 10.5194/acp-15-99-2015, 2015b.
647 Jiang, Z., Worden, J. R., Payne, V. H., Zhu, L. Y., Fischer, E., Walker, T., and Jones,
648 D. B. A.: Ozone export from East Asia: The role of PAN, J. Geophys. Res.-Atmos.,
649 121, 6555-6563, 10.1002/2016jd024952, 2016.
650 Kuhns, H., Knipping, E. M., and Vukovich, J. M.: Development of a United States-
651 Mexico emissions inventory for the Big Bend Regional Aerosol and Visibility
652 Observational (BRAVO) Study, Journal of the Air & Waste Management
653 Association, 55, 677-692, 2005.
654 Kopacz, M., Jacob, D. J., Fisher, J. A., Logan, J. A., Zhang, L., Megretskaia, I. A.,
655 Yantosca, R. M., Singh, K., Henze, D. K., Burrows, J. P., Buchwitz, M., Khlystova,
656 I., McMillan, W. W., Gille, J. C., Edwards, D. P., Eldering, A., Thouret, V., and
657 Nedelec, P.: Global estimates of CO sources with high resolution by adjoint
658 inversion of multiple satellite datasets (MOPITT, AIRS, SCIAMACHY, TES),
659 Atmospheric Chemistry and Physics, 10, 855-876, 2010.
660 Li, B. G., Gasser, T., Ciais, P., Piao, S. L., Tao, S., Balkanski, Y., Hauglustaine, D.,
661 Boisier, J. P., Chen, Z., Huang, M. T., Li, L. Z., Li, Y., Liu, H. Y., Liu, J. F., Peng,
662 S. S., Shen, Z. H., Sun, Z. Z., Wang, R., Wang, T., Yin, G. D., Yin, Y., Zeng, H.,
663 Zeng, Z. Z., and Zhou, F.: The contribution of China's emissions to global climate
664 forcing, Nature, 531, 357-361, 10.1038/nature17165, 2016a.
665 Li, J., Yang, W. Y., Wang, Z. F., Chen, H. S., Hu, B., Li, J. J., Sun, Y. L., Fu, P. Q.,
666 and Zhang, Y. Q.: Modeling study of surface ozone source-receptor relationships
667 in East Asia, Atmospheric Research, 167, 77-88, 10.1016/j.atmosres.2015.07.010,
668 2016b.

669 Li, M., Zhang, Q., Kurokawa, J., Woo, J. H., He, K. B., Lu, Z. F., Ohara, T., Song, Y.,
670 Streets, D. G., Carmichael, G. R., Cheng, Y. F., Hong, C. P., Huo, H., Jiang, X. J.,
671 Kang, S. C., Liu, F., Su, H., and Zheng, B.: MIX: a mosaic Asian anthropogenic
672 emission inventory under the international collaboration framework of the MICS-
673 Asia and HTAP, Atmospheric Chemistry and Physics, 17, 935-963, 10.5194/acp-
674 17-935-2017, 2017.
675 Li, X. Y., Liu, J. F., Mauzerall, D. L., Emmons, L. K., Walters, S., Horowitz, L. W.,
676 and Tao, S.: Effects of trans-Eurasian transport of air pollutants on surface ozone
677 concentrations over Western China, J. Geophys. Res.-Atmos., 119, 12338-12354,
678 10.1002/2014jd021936, 2014.
679 Liang, Q., Jaegle, L., Jaffe, D. A., Weiss-Penzias, P., Heckman, A., and Snow, J. A.:
680 Long-range transport of Asian pollution to the northeast Pacific: Seasonal
681 variations and transport pathways of carbon monoxide, J. Geophys. Res.-Atmos.,
682 109, 20, 10.1029/2003jd004402, 2004.
683 Lin, J.-T., Wuebbles, D. J., and Liang, X.-Z.: Effects of intercontinental transport on
684 surface ozone over the United States: Present and future assessment with a global
685 model, Geophysical Research Letters, 35, 10.1029/2007gl031415, 2008.
686 Lin, J.-T., Pan, D., Davis, S. J., Zhang, Q., He, K., Wang, C., Streets, D. G., Wuebbles,
687 D. J., and Guan, D.: China's international trade and air pollution in the United
688 States, Proceedings of the National Academy of Sciences, 111, 1736-1741,
689 10.1073/pnas.1312860111, 2014.
690 Lin, J. T., and McElroy, M. B.: Impacts of boundary layer mixing on pollutant vertical
691 profiles in the lower troposphere: Implications to satellite remote sensing,
692 Atmospheric Environment, 44, 1726-1739, 10.1016/j.atmosenv.2010.02.009,
693 2010.
694 Lin, J. T., Liu, Z., Zhang, Q., Liu, H., Mao, J., and Zhuang, G.: Modeling uncertainties
695 for tropospheric nitrogen dioxide columns affecting satellite-based inverse
696 modeling of nitrogen oxides emissions, Atmospheric Chemistry and Physics, 12,
697 12255-12275, 10.5194/acp-12-12255-2012, 2012a.
698 Lin, J. T., Tong, D., Davis, S., Ni, R. J., Tan, X. X., Pan, D., Zhao, H. Y., Lu, Z. F.,
699 Streets, D., Feng, T., Zhang, Q., Yan, Y. Y., Hu, Y. Y., Li, J., Liu, Z., Jiang, X. J.,
700 Geng, G. N., He, K. B., Huang, Y., and Guan, D. B.: Global climate forcing of
701 aerosols embodied in international trade, Nature Geoscience, 9, 790-794,
702 10.1038/ngeo2798, 2016.
703 Lin, M., Fiore, A. M., Horowitz, L. W., Cooper, O. R., Naik, V., Holloway, J., Johnson,
704 B. J., Middlebrook, A. M., Oltmans, S. J., Pollack, I. B., Ryerson, T. B., Warner,
705 J. X., Wiedinmyer, C., Wilson, J., and Wyman, B.: Transport of Asian ozone
706 pollution into surface air over the western United States in spring, J. Geophys.
707 Res.-Atmos., 117, D00v07, 10.1029/2011jd016961, 2012b.
708 Lin, W., Xu, X., Zheng, X., Dawa, J., Baima, C., and Ma, J.: Two-year measurements
709 of surface ozone at Dangxiong, a remote highland site in the Tibetan Plateau,
710 Journal of Environmental Sciences, 31, 133-145,
711 https://doi.org/10.1016/j.jes.2014.10.022, 2015.

712 Lin, W. L., Xu, X. B., Ge, B. Z., and Zhang, X. C.: Characteristics of gaseous pollutants
713 at Gucheng, a rural site southwest of Beijing, J. Geophys. Res.-Atmos., 114, 17,
714 10.1029/2008jd010339, 2009.
715 Liu, Z., Wang, Y. H., Gu, D. S., Zhao, C., Huey, L. G., Stickel, R., Liao, J., Shao, M.,
716 Zhu, T., Zeng, L. M., Liu, S. C., Chang, C. C., Amoroso, A., and Costabile, F.:
717 Evidence of Reactive Aromatics As a Major Source of Peroxy Acetyl Nitrate over
718 China, Environmental Science & Technology, 44, 7017-7022, 10.1021/es1007966,
719 2010.
720 Ma, J., Lin, W. L., Zheng, X. D., Xu, X. B., Li, Z., and Yang, L. L.: Influence of air
721 mass downward transport on the variability of surface ozone at Xianggelila
722 Regional Atmosphere Background Station, southwest China, Atmospheric
723 Chemistry and Physics, 14, 5311-5325, 10.5194/acp-14-5311-2014, 2014.
724 Mao, J. Q., Paulot, F., Jacob, D. J., Cohen, R. C., Crounse, J. D., Wennberg, P. O.,
725 Keller, C. A., Hudman, R. C., Barkley, M. P., and Horowitz, L. W.: Ozone and
726 organic nitrates over the eastern United States: Sensitivity to isoprene chemistry,
727 J. Geophys. Res.-Atmos., 118, 11256-11268, 10.1002/jgrd.50817, 2013.
728 Marenco, A., Thouret, V., Nedelec, P., Smit, H., Helten, M., Kley, D., Karcher, F.,
729 Simon, P., Law, K., Pyle, J., Poschmann, G., Von Wrede, R., Hume, C., and Cook,
730 T.: Measurement of ozone and water vapor by Airbus in-service aircraft: The
731 MOZAIC airborne program, An overview, J. Geophys. Res.-Atmos., 103, 25631-
732 25642, 10.1029/98jd00977, 1998.
733 McLinden, C. A., Olsen, S. C., Hannegan, B., Wild, O., Prather, M. J., and Sundet, J.:
734 Stratospheric ozone in 3-D models: A simple chemistry and the cross-tropopause
735 flux, J. Geophys. Res.-Atmos., 105, 14653-14665, 10.1029/2000jd900124, 2000.
736 Moorthi, S., and Suarez, M. J.: Relaxed Arakawa-Schubert. A Parameterization of
737 Moist Convection for General Circulation Models, Monthly Weather Review, 120,
738 978-1002, 1992.
739 Murray, L. T., Jacob, D. J., Logan, J. A., Hudman, R. C., and Koshak, W. J.: Optimized
740 regional and interannual variability of lightning in a global chemical transport
741 model constrained by LIS/OTD satellite data, J. Geophys. Res.-Atmos., 117, 14,
742 10.1029/2012jd017934, 2012.
743 Ott, L. E., Pickering, K. E., Stenchikov, G. L., Allen, D. J., DeCaria, A. J., Ridley, B.,
744 Lin, R. F., Lang, S., and Tao, W. K.: Production of lightning NOx and its vertical
745 distribution calculated from three-dimensional cloud-scale chemical transport
746 model simulations, J. Geophys. Res.-Atmos., 115, 19, 10.1029/2009jd011880,
747 2010.
748 Simone, N. W., Stettler, M. E. J., and Barrett, S. R. H.: Rapid estimation of global
749 civil aviation emissions with uncertainty quantification, Transport. Res. D-Tr. E.,
750 25, 33–41, doi:10.1016/j.trd.2013.07.001, 2013.
751 van der Werf, G. R., Randerson, J. T., Giglio, L., Collatz, G. J., Mu, M., Kasibhatla, P.
752 S., Morton, D. C., DeFries, R. S., Jin, Y., and van Leeuwen, T. T.: Global fire
753 emissions and the contribution of deforestation, savanna, forest, agricultural, and
754 peat fires (1997-2009), Atmospheric Chemistry and Physics, 10, 11707-11735,
755 10.5194/acp-10-11707-2010, 2010.

Verstraeten, W. W., Neu, J. L., Williams, J. E., Bowman, K. W., Worden, J. R., and Boersma, K. F.: Rapid increases in tropospheric ozone production and export from China (vol 8, pg 690, 2015), Nature Geoscience, 9, 643-643, 10.1038/ngeo2768, 2016.

Wang, T., Ding, A. J., Gao, J., and Wu, W. S.: Strong ozone production in urban plumes from Beijing, China, Geophysical Research Letters, 33, 5, 10.1029/2006gl027689, 2006.

Wang, Y., Zhang, Y., Hao, J., and Luo, M.: Seasonal and spatial variability of surface ozone over China: contributions from background and domestic pollution, Atmospheric Chemistry and Physics, 11, 3511-3525, 10.5194/acp-11-3511-2011, 2011.

Wang, Y., Konopka, P., Liu, Y., Chen, H., Muller, R., Ploger, F., Riese, M., Cai, Z., and Lu, D.: Tropospheric ozone trend over Beijing from 2002-2010: ozonesonde measurements and modeling analysis, Atmospheric Chemistry and Physics, 12, 8389-8399, 10.5194/acp-12-8389-2012, 2012.

Wang, Y. H., Jacob, D. J., and Logan, J. A.: Global simulation of tropospheric O-3-NOx-hydrocarbon chemistry 1. Model formulation, J. Geophys. Res.-Atmos., 103, 10713-10725, 10.1029/98jd00158, 1998.

Wu, R. R., Bo, Y., Li, J., Li, L. Y., Li, Y. Q., and Xie, S. D.: Method to establish the emission inventory of anthropogenic volatile organic compounds in China and its application in the period 2008-2012, Atmospheric Environment, 127, 244-254, 10.1016/j.atmosenv.2015.12.015, 2016.

Wu, S. L., Duncan, B. N., Jacob, D. J., Fiore, A. M., and Wild, O.: Chemical nonlinearities in relating intercontinental ozone pollution to anthropogenic emissions, Geophysical Research Letters, 36, 5, 10.1029/2008gl036607, 2009.

Xia, Y. M., Zhao, Y., and Nielsen, C. P.: Benefits of of China's efforts in gaseous pollutant control indicated by the bottom-up emissions and satellite observations 2000-2014, Atmospheric Environment, 136, 43-53, 10.1016/j.atmosenv.2016.04.013, 2016.

Xu, W., Lin, W., Xu, X., Tang, J., Huang, J., Wu, H., and Zhang, X.: Long-term trends of surface ozone and its influencing factors at the Mt Waliguan GAW station, China – Part 1: Overall trends and characteristics, Atmos. Chem. Phys., 16, 6191-6205, 10.5194/acp-16-6191-2016, 2016.

Xu, W., Lin, W., Xu, X., Tang, J., Huang, J., Wu, H., and Zhang, X.: Long-term trends of surface ozone and its influencing factors at the Mt Waliguan GAW station, China – Part 1: Overall trends and characteristics, Atmos. Chem. Phys., 16, 6191-6205, https://doi.org/10.5194/acp-16-6191-2016, 2016.

Xu, X., Lin, W., Wang, T., Yan, P., Tang, J., Meng, Z., and Wang, Y.: Long-term trend of surface ozone at a regional background station in eastern China 1991-2006: enhanced variability, Atmospheric Chemistry and Physics, 8, 2595-2607, 2008.

Xue, L. K., Wang, T., Zhang, J. M., Zhang, X. C., Deliger, Poon, C. N., Ding, A. J., Zhou, X. H., Wu, W. S., Tang, J., Zhang, Q. Z., and Wang, W. X.: Source of surface ozone and reactive nitrogen speciation at Mount Waliguan in western

China: New insights from the 2006 summer study, Journal of Geophysical Research: Atmospheres, 116, n/a-n/a, 10.1029/2010JD014735, 2011.

Xue, L. K., Wang, T., Gao, J., Ding, A. J., Zhou, X. H., Blake, D. R., Wang, X. F., Saunders, S. M., Fan, S. J., Zuo, H. C., Zhang, Q. Z., and Wang, W. X.: Ground-level ozone in four Chinese cities: precursors, regional transport and heterogeneous processes, Atmospheric Chemistry and Physics, 14, 13175-13188, 10.5194/acp-14-13175-2014, 2014.

Yan, Y., Lin, J., Chen, J., and Hu, L.: Improved simulation of tropospheric ozone by a global-multi-regional two-way coupling model system, Atmospheric Chemistry and Physics, 16, 2381-2400, 10.5194/acp-16-2381-2016, 2016.

Yan, Y., Lin, J., and He, C.: Ozone trends over the United States at different times of day, Atmos. Chem. Phys. Discuss., https://doi.org/10.5194/acp-2017-659, in review, 2017a.

Yan, Y., Pozzer, A., Ojha, N., Lin, J., and Lelieveld, J.: Analysis of European ozone trends in the period 1995–2014, Atmos. Chem. Phys. Discuss., https://doi.org/10.5194/acp-2017-1077, in review, 2017b.

Yan, Y. Y., Lin, J. T., Kuang, Y., Yang, D., and Zhang, L.: Tropospheric carbon monoxide over the Pacific during HIPPO: two-way coupled simulation of GEOS-Chem and its multiple nested models, Atmospheric Chemistry and Physics, 14, 12649-12663, 10.5194/acp-14-12649-2014, 2014.

Yin, X. F., Kang, S. C., de Foy, B., Cong, Z. Y., Luo, J. L., Zhang, L., Ma, Y. M., Zhang, G. S., Rupakheti, D., and Zhang, Q. G.: Surface ozone at Nam Co in the inland Tibetan Plateau: variation, synthesis comparison and regional representativeness, Atmospheric Chemistry and Physics, 17, 11293-11311, 10.5194/acp-17-11293-2017, 2017.

Young, P. J., Archibald, A. T., Bowman, K. W., Lamarque, J. F., Naik, V., Stevenson, D. S., Tilmes, S., Voulgarakis, A., Wild, O., Bergmann, D., Cameron-Smith, P., Cionni, I., Collins, W. J., Dalsoren, S. B., Doherty, R. M., Eyring, V., Faluvegi, G., Horowitz, L. W., Josse, B., Lee, Y. H., MacKenzie, I. A., Nagashima, T., Plummer, D. A., Righi, M., Rumbold, S. T., Skeie, R. B., Shindell, D. T., Strode, S. A., Sudo, K., Szopa, S., and Zeng, G.: Pre-industrial to end 21st century projections of tropospheric ozone from the Atmospheric Chemistry and Climate Model Intercomparison Project (ACCMIP), Atmospheric Chemistry and Physics, 13, 2063-2090, 10.5194/acp-13-2063-2013, 2013.

Zhang, L., Jacob, D. J., Boersma, K. F., Jaffe, D. A., Olson, J. R., Bowman, K. W., Worden, J. R., Thompson, A. M., Avery, M. A., Cohen, R. C., Dibb, J. E., Flock, F. M., Fuelberg, H. E., Huey, L. G., McMillan, W. W., Singh, H. B., and Weinheimer, A. J.: Transpacific transport of ozone pollution and the effect of recent Asian emission increases on air quality in North America: an integrated analysis using satellite, aircraft, ozonesonde, and surface observations, Atmospheric Chemistry and Physics, 8, 6117-6136, 2008.

Zhang, Q., Streets, D. G., Carmichael, G. R., He, K. B., Huo, H., Kannari, A., Klimont, Z., Park, I. S., Reddy, S., Fu, J. S., Chen, D., Duan, L., Lei, Y., Wang, L. T., and Yao, Z. L.: Asian emissions in 2006 for the NASA INTEX-B mission,

Atmos. Chem. Phys., 9, 5131–5153, doi:10.5194/acp-9-5131-2009, 2009.

Zhang, Q., Jiang, X. J., Tong, D., Davis, S. J., Zhao, H. Y., Geng, G. N., Feng, T., Zheng, B., Lu, Z. F., Streets, D. G., Ni, R. J., Brauer, M., van Donkelaar, A., Martin, R. V., Huo, H., Liu, Z., Pan, D., Kan, H. D., Yan, Y. Y., Lin, J. T., He, K. B., and Guan, D. B.: Transboundary health impacts of transported global air pollution and international trade, Nature, 543, 705-709, 10.1038/nature21712, 2017.

Zhao, B., Wang, S. X., Liu, H., Xu, J. Y., Fu, K., Klimont, Z., Hao, J. M., He, K. B., Cofala, J., and Amann, M.: NOx emissions in China: historical trends and future perspectives, Atmos. Chem. Phys., 13, 9869-9897, 10.5194/acp-13-9869-2013, 2013.

Zhu, B., Hou, X. W., and Kang, H. Q.: Analysis of the seasonal ozone budget and the impact of the summer monsoon on the northeastern Qinghai-Tibetan Plateau, J. Geophys. Res.-Atmos., 121, 2029-2042, 10.1002/2015jd023857, 2016.

Atmos. Chem. Phys. Discuss., https://doi.org/10.5194/acp-2017-1226
Manuscript under review for journal Atmos. Chem. Phys.
Discussion started: 16 January 2018

Atmospheric Chemistry and Physics Discussions

858 Table 1. Emissions used in the model.

Region	Inventory	Resolution [a]	Year	Species [b]	References & Notes
Anthropogenic emissions					
Global	EDGAR v4.2	0.1 °x 0.1 °, monthly	2008	NOx, SO2, CO, NH3	http://edgar.jrc.ec.europa.eu/overview.php?v=42
Global	BOND	1 °x 1 °, monthly	2000	BC and OC	Bond et al. (2007)
Global	RETRO	0.5 °x 0.5 °, monthly	2000	NMVOC	ftp://ftp.retro.enes.org/pub/emissions/aggregated/anthro/0.5x0.5/2000/
Global	ICOADS, shipping	1 °x 1 °, monthly	2002	NOx, SO2, CO	Wang et al. (2008); http://coast.cms.udel.edu/GlobalShipEmissions/
Global	AEIC, aircraft	1 °x 1 °, annual	2005	NOx, SO2, CO, NMVOC, BC, OC	Simone et al. (2013)
Asia	INTEX-B	1 °x 1 °, monthly	2006	NOx, SO2, CO, NMVOC, BC, OC, NH3	Zhang et al. (2009). NH3 only available for 2000.
China	MEIC	0.25 °x 0.25 °, monthly	2008	NOx, SO2, CO, NMVOC, NH3	Li et al. (2017); Geng et al. (2017); http://www.meicmodel.org/.
United States	NEI2005	4km x 4km, monthly & weekend/weekday	2005 [c]	NOx, SO2, CO, NMVOC, NH3, BC, OC	ftp://aftp.fsl.noaa.gov/divisions/taq/emissions_data_2005
Canada	CAC	1 °x 1 °, annual	2008	NOx, SO2, CO, NH3	http://www.ec.gc.ca/pdb/cac/cac_home_e.cfm
Mexico	BRAVO	1 °x 1 °, annual	1999 [c]	NOx, SO2, CO	Kuhns et al. (2005)
Europe	EMEP	1 °x 1 °, monthly	2007	NOx, SO2, CO	Auvray and Bey (2005); http://www.emep.int/index.html
Biomass burning emissions					
Global	GFED3	0.5 °x 0.5 °, daily	2008	NOx, SO2, CO, NMVOC, NH3, BC, OC	van der Werf et al., 2010; http://www.globalfiredata.org
Natural/Semi-natural emissions (online calculation)					
Global	MEGAN v2.1	Model resolution	2008	ISOP, monoterpenes, sesquiterpenes, MOH, ACET, ETOH, CH2O, ALD2, HCOOH, C2H4, TOLU, PRPE	Guenther et al. (2012)
Global	Soil NOx	Model resolution	2008	NO	Hudman et al. (2012)
Global	Lightning NOx	Model resolution	2008	NO	Murray et al. (2012)

859 a. Before re-gridded to model horizontal resolutions. For more information, see
860 http://wiki.seas.harvard.edu/geos-chem/index.php/Anthropogenic_emissions.

861 b. Notes for NMVOC: RETRO includes PRPE, C3H8, ALK4, ALD2, CH2O and
862 MEK; in the CTM, MEK emissions are further allocated to MEK (25%) and ACET
863 (75%). AEIC, INTEX-B and MEIC include PRPE, C2H6, C3H8, ALK4, ALD2,
864 CH2O, MEK and ACET. NEI05 includes PRPE, C3H8, ALK4, CH2O, MEK and

ACET. EMEP includes PRPE, ALK4, ALD2 and MEK. Emissions of C2H6 outside Asia are from Xiao et al. (2008).

c. Over the United States and Mexico, emissions of CO, NOx are scaled to 2008 and 2006 respectively. (http://wiki.seas.harvard.edu/geos-chem/index.php/Scale_factors_for_anthropogenic_emissions).

Atmos. Chem. Phys. Discuss., https://doi.org/10.5194/acp-2017-1226
Manuscript under review for journal Atmos. Chem. Phys.
Discussion started: 16 January 2018

870 Table 2. Model simulations.

Full chemistry simulation	Description	Tagged ozone simulation	Description
CTL	Full-chemistry simulation with all emissions	T_CTL	Driven by daily ozone production and loss rate archived from CTL
xANTH	Without global anthropogenic emissions	T_xANTH	With respect to xANTH
xCH	Without anthropogenic emissions of China	T_xCH	With respect to xCH
xJAKO	Without anthropogenic emissions of Japan and Korea	T_xJAKO	With respect to xJAKO
xSEA	Without anthropogenic emissions of South-East Asia	T_xSEA	With respect to xSEA
xSA	Without anthropogenic emissions of South Asia	T_xSA	With respect to xSA
xROA	Without anthropogenic emissions of Rest of Asia	T_xROA	With respect to xROA
xEU	Without anthropogenic emissions of Europe	T_xEU	With respect to xEU
xNA	Without anthropogenic emissions of North America	T_xNA	With respect to xNA
xROW	Without anthropogenic emissions of Rest of World	T_xROW	With respect to xROW

871

Atmos. Chem. Phys. Discuss., https://doi.org/10.5194/acp-2017-1226
Manuscript under review for journal Atmos. Chem. Phys.
Discussion started: 16 January 2018

872 Table 3. Comparison of simulated and observed springtime MDA8 ozone and CO at
873 five regional background sites in China and six global background stations nearby
874 China with hourly measurements.

Country	Site	Location	Year	MDA8 Ozone			CO		
				Obs (ppb)	Model (ppb)	NMB (%)	Obs (ppb)	Model (ppb)	NMB (%)
China	Gucheng	39.1 °N, 115.7 °E, 15m	2007	48.8	50.2	2.9			
	Longfengshan	44.7 °N, 127.6 °E, 331m	2007	50.6	52.9	4.5	290	251	-13.4
	Lin'an	30.2 °N, 119.7 °E, 132m	2008	65.1	68.9	5.8	628	418	-33.4
	Shangri-La	28.0 °N, 99.4 °E, 3580m	2008	61.4	68.7	11.9	181	139	-23.2
	Waliguan	36.3 °N, 100.9 °E, 3816m	2008	56.5	64.4	14.0			
Kyrgyzstan	Issyk-Kul	42.6 °N, 77.0 °E, 1640m	2008	52.8	59.0	11.7			
Nepal	Everest-Pyramid	28.0 °N, 86.8 °E, 5079m	2008	66.3	79.1	19.3			
Indonesia	Bukit Koto Tabang	0.2 °S, 100.3 °E, 865m	2008				141	146	3.5
Japan	Yonagunijima	24.5 °N, 123.0 °E, 30m	2008	54.8	56.4	2.9	208	157	-24.5
	Tsukuba	36.1 °N, 140.1 °E, 25m	2008	47.2	56.0	18.6			
	Ryori	39.0 °N, 141.8 °E, 260m	2008	54.6	54.7	0.2	211	203	-3.8

875

Atmos. Chem. Phys. Discuss., https://doi.org/10.5194/acp-2017-1226
Manuscript under review for journal Atmos. Chem. Phys.
Discussion started: 16 January 2018

Atmospheric Chemistry and Physics Discussions

876 Table 4. Comparison of simulated springtime monthly mean ozone with observations
877 from EANET and literature.

Country	Site	Year	Location	Characteristics	Obs (ppb)	Model (ppb)	NMB (%)
Japan (EANET)	Rishiri	2008	45.5 °N, 141.2 °E, 40m	Remote	55.0	46.0	-16.5
	Ochiishi	2008	43.1 °N, 145.5 °E, 49m	Remote	48.4	46.7	-3.6
	Tappi	2008	41.3 °N, 140.4 °E, 105m	Remote	66.2	48.8	-26.2
	Sado-seki	2008	38.2 °N, 138.4 °E, 136m	Remote	61.3	53.3	-13.0
	Happo	2008	36.7 °N, 137.8 °E, 1850m	Remote	62.0	53.8	-13.2
	Ijira	2008	35.6 °N, 136.7 °E, 140m	Rural	30.7	47.8	55.7
	Oki	2008	36.3 °N, 133.2 °E, 90m	Remote	58.8	55.7	-5.3
	Banryu	2008	34.7 °N, 131.8 °E, 53m	Urban	48.5	52.1	7.5
	Yusuhara	2008	33.4 °N, 132.9 °E, 790m	Remote	53.7	53.1	-1.1
	Hedo	2008	26.9 °N, 128.3 °E, 60m	Remote	53.6	54.2	1.1
	Ogasawara	2008	27.1 °N, 142.2 °E, 230m	Remote	37.9	41.1	8.3
Republic of Korea (EANET)	Kanghwa	2008	37.7 °N, 126.3 °E, 150m	Rural	52.3	47.4	-9.4
	Cheju	2008	33.3 °N, 126.2 °E, 72m	Remote	56.3	57.7	2.5
	Imsil	2008	35.6 °N, 127.2 °E	Rural	30.3	48.2	58.8
Russia (EANET)	Mondy	2008	51.7 °N, 101.0 °E, 2000m	Remote	43.0	49.2	14.4
China (literature)	Miyun	2006	40.5 °N, 116.8 °E, 152m	Rural	48.7	35.3	-27.4
	Mt. Tai	2004-2005	24.25 °N, 117.10 °E, 1533m	Rural	57.0	54.8	-3.9
	Mt. Hua	2004-2005	34.49 °N, 110.09 °E, 2064m	Rural	50.0	51.8	3.5
	Mt. Huang	2004-2005	30.13 °N, 118.15 °E, 1836m	Rural	59.3	54.0	-9.0
	Hong Kong	1994-2007	22.2 °N, 114.2 °E, 60m	Rural	36.0	53.4	48.2
	Nanjing	2000-2002	32.1 °N, 118.7 °E	Urban	27.0	31.3	16.0

878

Atmos. Chem. Phys. Discuss., https://doi.org/10.5194/acp-2017-1226
Manuscript under review for journal Atmos. Chem. Phys.
Discussion started: 16 January 2018

Atmospheric Chemistry and Physics Discussions

879 Table 5. Springtime anthropogenic emissions of NOx, CO and NMVOC of each
880 region defined in Fig. 1.

	China	Japan and Korea	South-East Asia	South Asia	Rest of Asia	Europe	North America	Rest of world
NOx (TgN)	2.0	0.3	0.4	0.4	0.7	1.2	1.3	1.0
CO (Tg)	42.3	16.7	10.9	16.7	10.0	12.5	17.7	25.5
NMVOC	2.9	0.2	1.3	1.3	1.1	1.1	2.1	1.9

881

Atmos. Chem. Phys. Discuss., https://doi.org/10.5194/acp-2017-1226
Manuscript under review for journal Atmos. Chem. Phys.
Discussion started: 16 January 2018

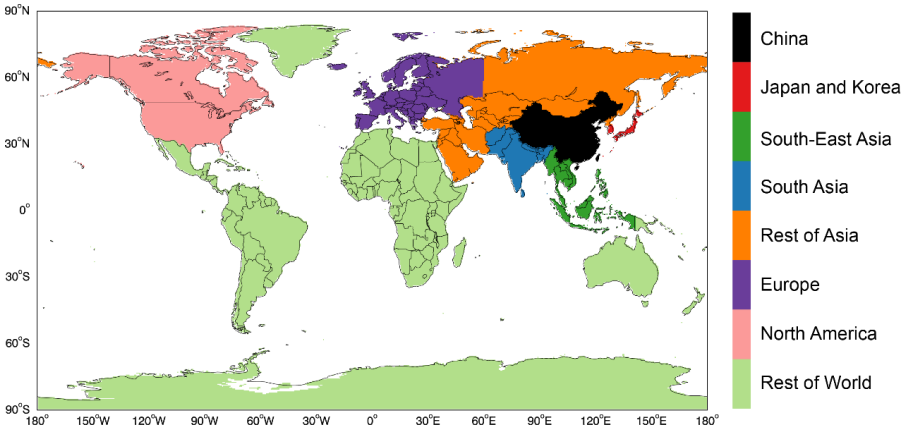

882

883 Figure 1. Eight emission source regions.

Atmos. Chem. Phys. Discuss., https://doi.org/10.5194/acp-2017-1226
Manuscript under review for journal Atmos. Chem. Phys.
Discussion started: 16 January 2018

Atmospheric Chemistry and Physics Discussions

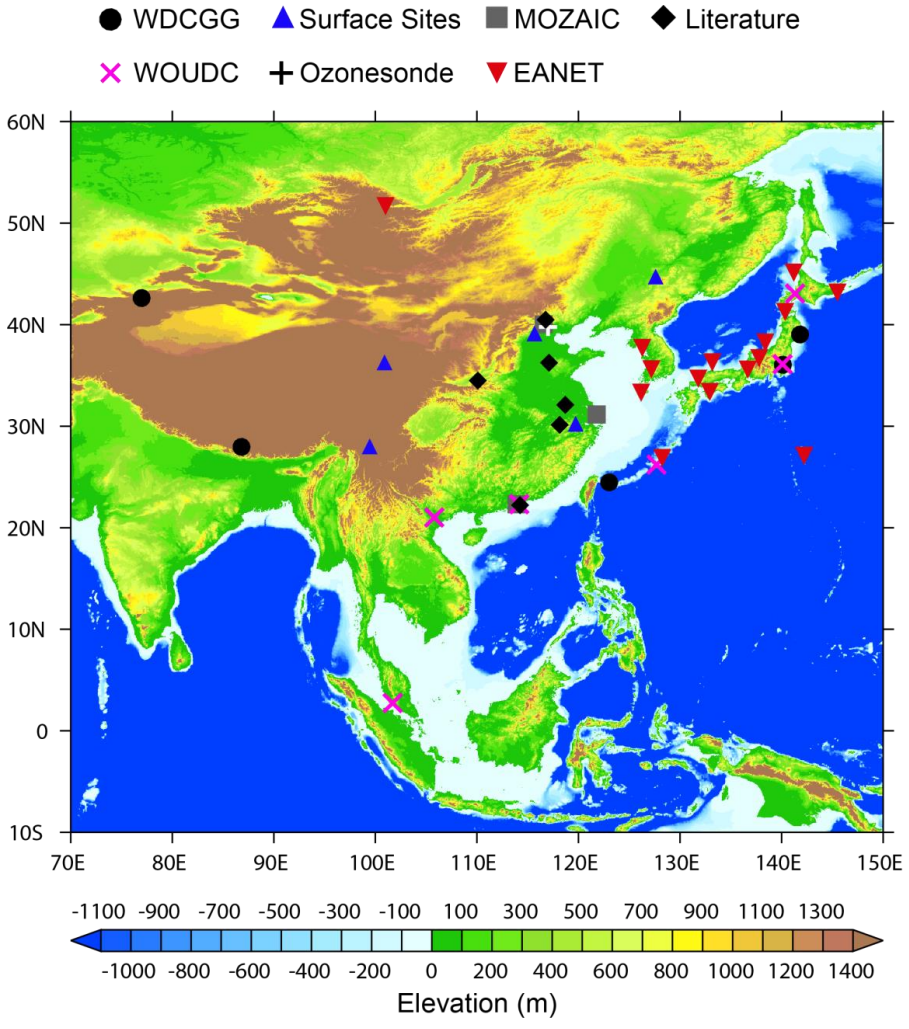

884

885 Figure 2. Observation sites overlaying upon the surface elevation map from the 2 min
886 Gridded Global Relief Data (ETOPO2v2) available at NGDC Marine Trackline
887 Geophysical database (http://www.ngdc.noaa.gov/mgg/global/etopo2.html).

Atmos. Chem. Phys. Discuss., https://doi.org/10.5194/acp-2017-1226
Manuscript under review for journal Atmos. Chem. Phys.
Discussion started: 16 January 2018

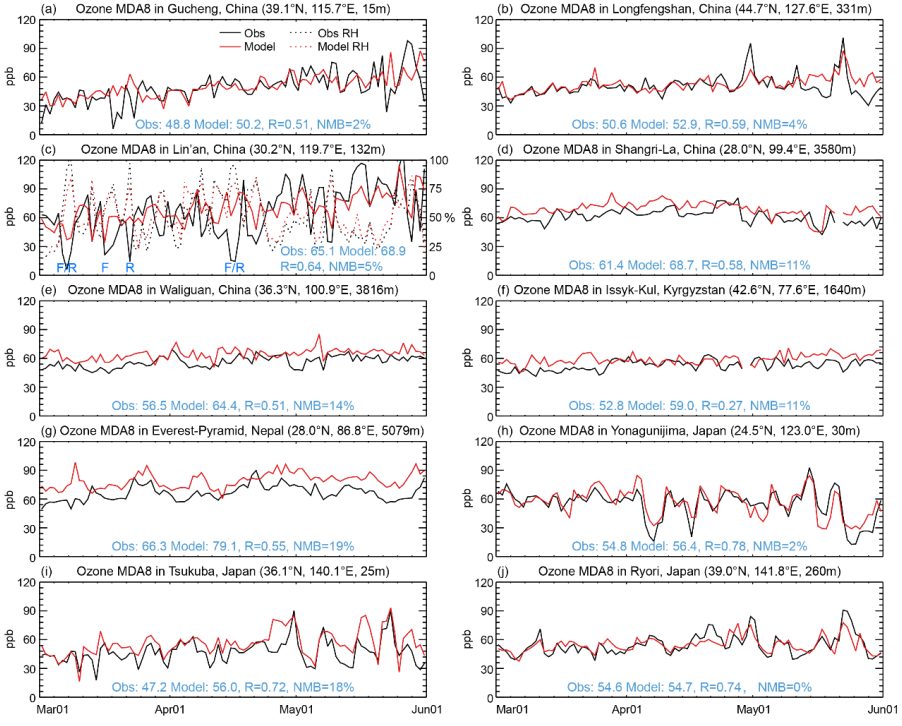

Figure 3. Time series of springtime MDA8 ozone at surface sites over (a–e) China and (f–j) nearby countries. Due to lack of measurement data in 2008, comparisons at Gucheng and Longfengshan are based in 2007. In (c), observed and modeled RH are also compared; and the "F" and "R" symbols denote observed frog or rain, respectively.

Atmos. Chem. Phys. Discuss., https://doi.org/10.5194/acp-2017-1226
Manuscript under review for journal Atmos. Chem. Phys.
Discussion started: 16 January 2018

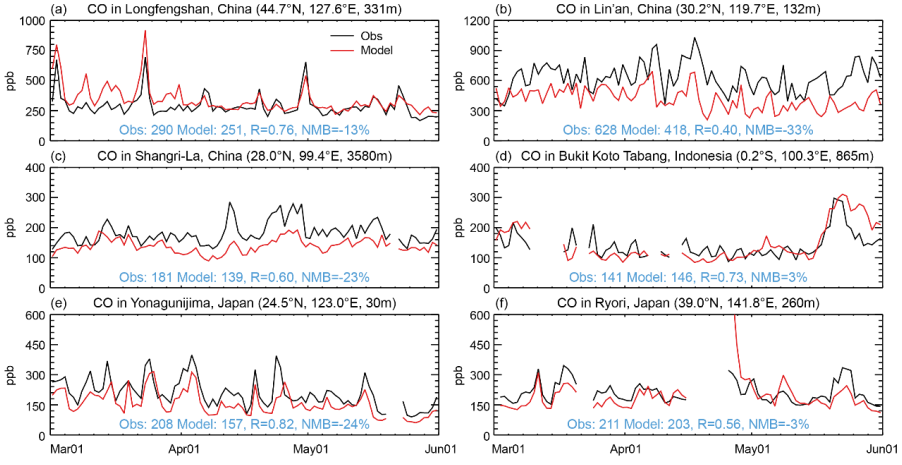

894

895 Figure 4. Time series of daily mean CO at six surface sites over (a–c) China and (d–f)
896 nearby countries.

Atmos. Chem. Phys. Discuss., https://doi.org/10.5194/acp-2017-1226
Manuscript under review for journal Atmos. Chem. Phys.
Discussion started: 16 January 2018

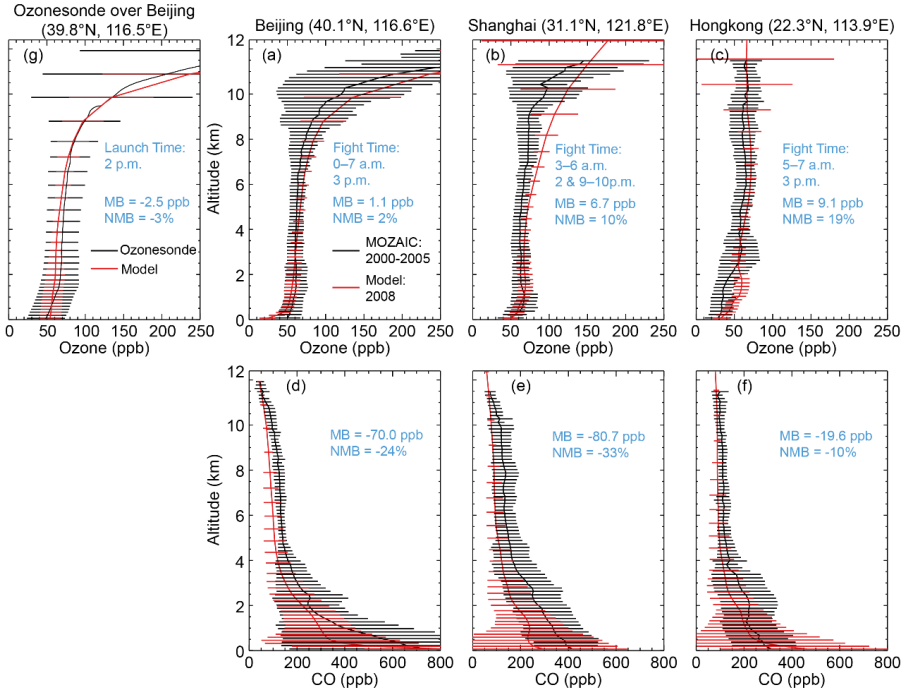

Figure 5. Model and MOZAIC vertical profiles of (a–c) ozone and (d–f) CO over airports of Beijing, Shanghai and Hong Kong, averaged over multiple profiles. (g) Model and GPSO3 ozonesonde data over Beijing in spring 2008. Horizontal bars indicate 1 standard deviation across multiple profiles. Mean bias (MB), normalized mean bias (NMB), main fight times (local time) at each MOZAIC site and GPSO3 ozonesonde launch time (local time) are also shown.

Atmos. Chem. Phys. Discuss., https://doi.org/10.5194/acp-2017-1226
Manuscript under review for journal Atmos. Chem. Phys.
Discussion started: 16 January 2018

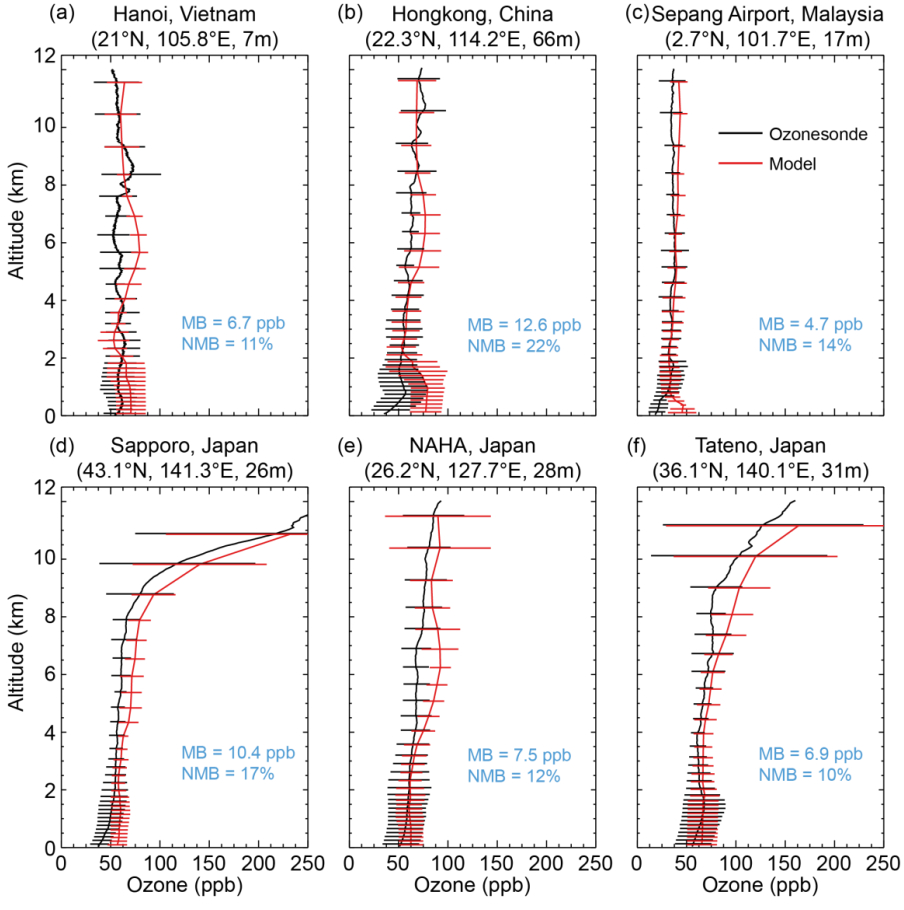

Figure 6. Model and WOUDC ozone profiles at six sites, averaged over multiple profiles. Horizontal lines indicate 1 standard deviation across multiple profiles. Mean bias (MB) and normalized mean bias (NMB) are shown in blue.

Atmos. Chem. Phys. Discuss., https://doi.org/10.5194/acp-2017-1226
Manuscript under review for journal Atmos. Chem. Phys.
Discussion started: 16 January 2018

Atmospheric Chemistry and Physics Discussions

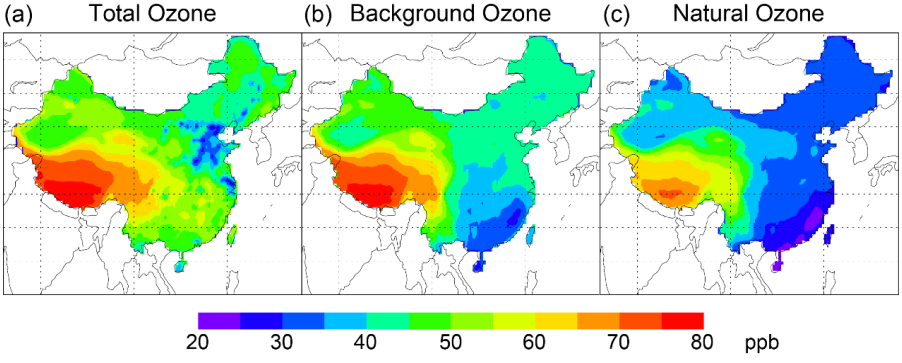

908

909 Figure 7. Spatial distribution of springtime daily mean (a) total surface ozone, (b)
910 background ozone and (c) natural ozone over China.

Atmos. Chem. Phys. Discuss., https://doi.org/10.5194/acp-2017-1226
Manuscript under review for journal Atmos. Chem. Phys.
Discussion started: 16 January 2018

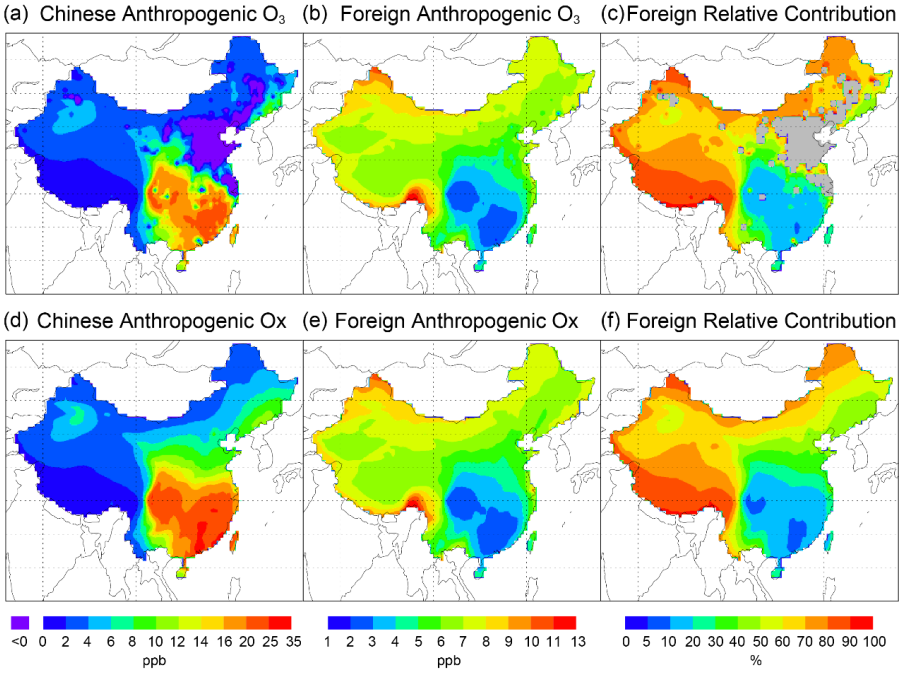

Figure 8. Spatial distribution of springtime daily mean surface ozone over China contributed by (a) domestic and (b) foreign anthropogenic emissions. (c) Percentage contribution of foreign anthropogenic emissions to total anthropogenic ozone; areas with negative Chinese contributions (due to NOx titration) are marked in grey. (d–f) Similar to (a–c) but for Ox (= O_3 + NO_2).

Atmos. Chem. Phys. Discuss., https://doi.org/10.5194/acp-2017-1226
Manuscript under review for journal Atmos. Chem. Phys.
Discussion started: 16 January 2018

Atmospheric Chemistry and Physics Discussions

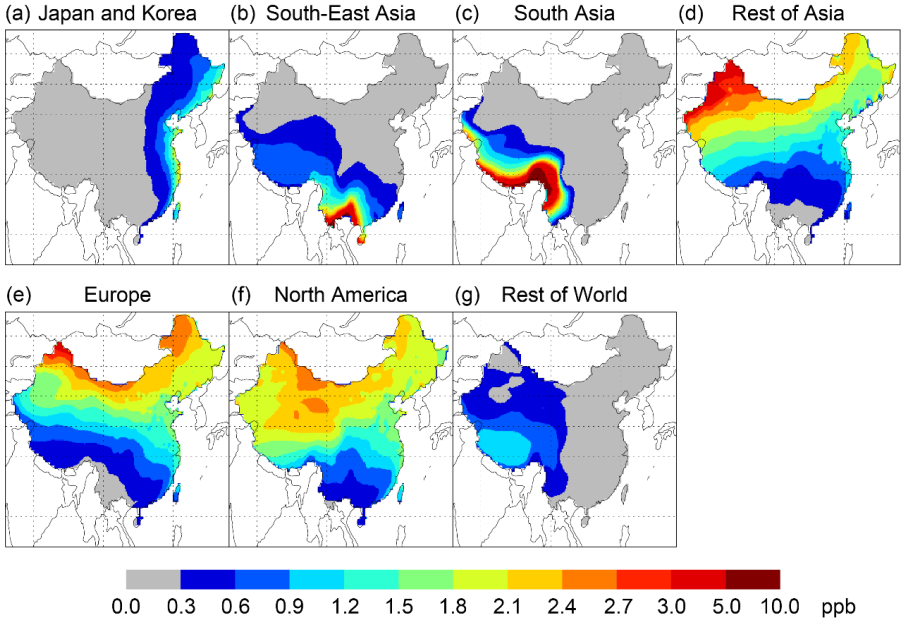

Figure 9. Spatial distribution of springtime daily mean surface ozone over China contributed by anthropogenic emissions of individual regions.

920

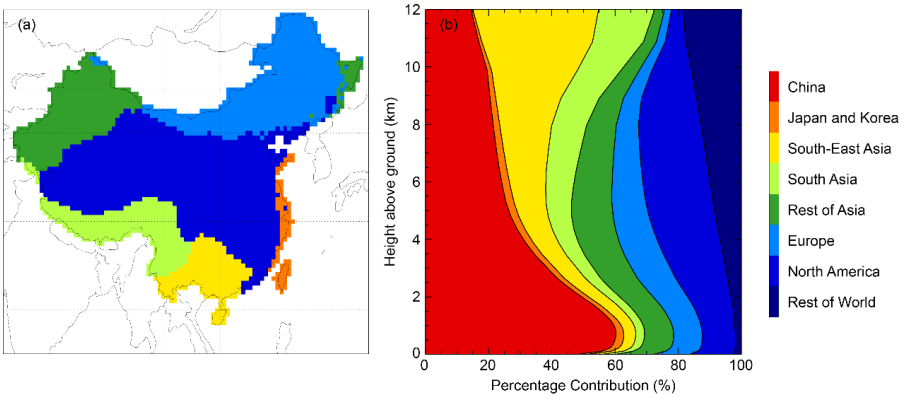

921

922 Figure 10. (a) Indication of the largest foreign anthropogenic contributor to surface
923 ozone at individual locations of China. (b) Vertical distribution of percentage
924 contribution of each region to total anthropogenic ozone over China.

Atmos. Chem. Phys. Discuss., https://doi.org/10.5194/acp-2017-1226
Manuscript under review for journal Atmos. Chem. Phys.
Discussion started: 16 January 2018

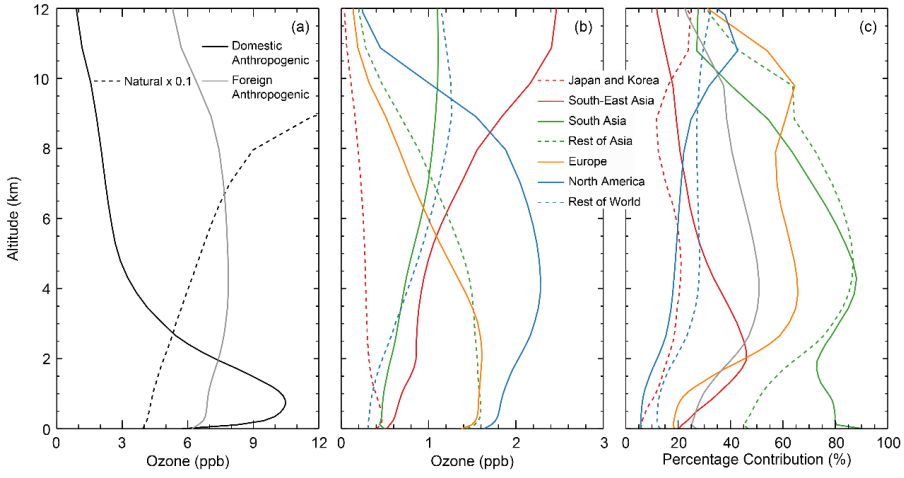

925

926 Figure 11. (a) Vertical distribution of China average daily mean ozone contributed by
927 domestic anthropogenic emissions, foreign anthropogenic emissions, and natural
928 sources (scaled by 0.1). (b) Contribution by anthropogenic emissions of each foreign
929 source region. (c) The portion of transboundary ozone over China produced within
930 each foreign source region's territory.